AL-QADISIYAH JOURNAL FOR ENGINEERING SCIENCES 13 (2020) 136–143

Contents lists available at http://qu.edu.iq

Al-Qadisiyah Journal for Engineering Sciences

Journal homepage: http://qu.edu.iq/journaleng/index.php/JQES

Numerical Study on the Performance of GFRP RC Beams Exposed to High Temperature

Nuha Hussien [a], ***Haitham Al-Thairy*** [a,*]

[a] *Civil Eng. Depart. / College of Eng./ University of Al-Qadisiyah, Iraq*

ARTICLE INFO

Article history:
Received 03 April 2020
Received in revised form 22 May 2020
Accepted 15 June 2020

Keywords:
Numerical simulation
GFRP-RC beams
High temperature
ABAQUS
Heating rate

ABSTRACT

This paper presents and validates a numerical model utilizing the nonlinear finite element software ABAQUS/Standard to simulate the performance and failure of Glass Fibre Reinforced Polymers reinforced concrete beams under high temperature. A numerical model was firstly developed by selecting the proper geometrical and material modeling parameters with suitable analysis procedures available in ABAQUS/Standard. The developed numerical model was verified by comparing numerical results with the corresponding results of the experimental test extracted from the current study on Glass Fibre reinforced concrete beams under different elevated temperatures ranges from (20 to 600ºC). Validation results have indicated the accuracy of the suggested numerical model. The validated numerical model was implemented to investigate the effect of important parameters on the performance and maximum load of Glass Fibre reinforced concrete beams under different elevated temperatures that are not considered in the current experimental tests. These parameters include the effect of exposure time or time-temperature history and effect of temperature distribution around the beams

1. Introduction

In building design, fire endurance is one of the major safety requirements. High-temperature effect on structures which are reinforced with FRP bars considered one of the more important factors of the design, although this factor has limited attention from the researchers with a limited number of research studies. However, the deterioration in the mechanical properties of FRP bars was investigated by several researches. Saafi [1] has established a general equation for the degradation in the mechanical properties of FRP material under different elevated temperatures. Saafi's equations have been used by a number of researches in the numerical simulation of FRP bars[2][3] (see **Figure 1)**.

Abbasi and Hogg [4] suggested two methods for predicting the effect of elevated temperature on some properties of glass fibre reinforced concrete beams. The two method was the suggested semi-empirical equation and FE model based on experimental studies conducted by Sakashita et al. [5] and Lin et al.[6] and Al-Baghdadi [7]. All beams were reinforced by FRP bars at the tension zone and exposed to ISO-834 standard fire curve [8].A whole concrete section with homogenous material was considered in finite

element model .While the thermal properties of concrete were taken as proposed by Abbasi [9] assuming no concrete cracking during the fire test.

* *Corresponding author.*
E-mail address: Haitham.althairy@qu.edu.iq (Haitham. Al-Thairy)

https://doi.org/10.30772/qjes.v13i2.635
2411-7773/

Nomenclature

ACI	American Concrete Institute
ASTM	American Society for Testing and Materials
C3D8R	Eight-node brick element with reduced integration
DC1D2	Two-node link heat transfer truss element
DC3D8	Eight-node liner heat transfer brick element
FEM	Finite Element Modeling
FRP	Fiber reinforced polymer
GFRP	Glass fiber reinforced polymer
GF	Fracture energy
RC	Reinforced Concrete
T3D2	Two-node truss element
W_1	Crack opinions at 0.15 of ultimate stress
W_O	Crack opinions at ultimate stress

In addition, GFRP RC beam with dimensions of (350mm width × 400mm height) and overall length of 4250 mm and concrete cover of 70mm was designed and simulated by using FE model. Comparison of time-temperature curves between the FE model and semi-empirical equation has shown that the FE model underestimates the time-temperature curve while the semi-empirical equation shows good agreements.

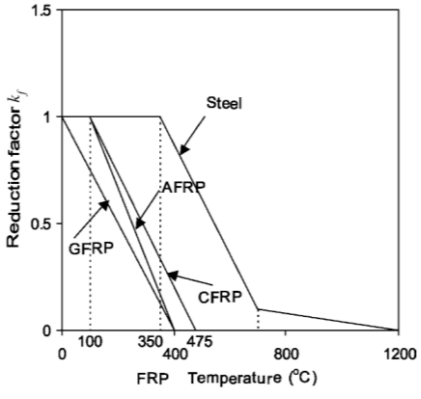

a) **Tensile strength**

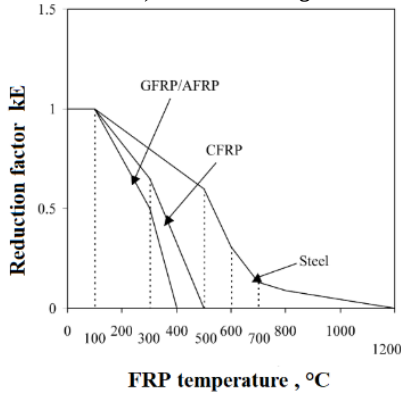

b) Elastic modulus

Figure 1 : Reduction factor of tensile strength and elastic modulus of various type of FRP bars [1]

Rafi et al. [10] have carried out finite element simulations of RC beams reinforced with CFRP bars under elevated temperature. The concrete was assumed to be isotropic and thermal conductivity and coefficient of thermal expansion was taken according to Eurocode 2[11] along with the mechanical properties of concrete at elevated temperature . In addition, the coefficient of thermal expansion of CFRP bars exposed to elevated temperature was assumed constant according to ACI440.1R-15 [12] while the mechanical properties of CFRP-bars under elevated temperature were taken from the equations suggested by Saafi [1]. However, numerical simulation results have shown large deviation from the experimental results.

Yu and Kodur [3] presented finite element analysis to evaluate the fire performance of concrete beam reinforced by FRP and steel bars. According to Eurocode 2[11] , ASCE standard [13] and insulation layout suggested by Bisby [14], heat transfer analysis and relevant high-temperature thermal properties of concrete was applied to establish temperature distribution over beam cross-section. Both specific heat and thermal conductivity of steel and FRP bars were not considered in the analysis due to the neglected effect of these properties on temperature distribution as suggested by Lie [15]. GFRP bars were analyzed according to models suggested by previously studies Saafi [1], Wang and Kodur [16], Bisby [14], FIB bulletin[17] and ACI 440.1R-15[12], which proposed a linear stress-strain curve up to failure and a reduction of tensile strength about 25% of GFRP bars under a temperature of 400 °C and 100% under a temperature of 1000 °C . Results of the numerical model have shown good agreement with measured data by Rafi and Nadjai [18] and Abbasi & Hogg [19]. The main conclusion extracted from this Yu and Kodur [3] study is that the load capacity of FRP-RC beams is less than the load capacity of Steel-RC beams under exposed to high temperature. Parametric studies were conducted and indicate a notable effect regarding the increasing of concrete cover thickness on the fire capacity of FRP-reinforced concrete beams. Also, the existing of axial restrain as well as provided FRP beams with fire endurances material reflect efficiency in increasing fire capacity.

The above-mentioned research studies have reflected the ability of finite element package ABAQUS in simulating the behavior and ultimate load of FRP reinforced concrete beams under exposure to elevated temperature with a very good accuracy .In addition, the stress-strain relationship of normal weight concrete at high temperature proposed by Eurocode 2[11]and Eurocode 4[20]was successfully used to predict the degradation of the concrete strength under high temperature. However, some of previous numerical models have not considered the degradation of FRP mechanical properties exposed to high temperature in there numerical simulations [21]. Saafi' equations was used in the numerical simulations of current numerical study [1] (see **Figure 1**). Therefore, the main object of the current study is to develop a more accurate numerical model to simulate the performance of GFRP-RC beams exposed to high temperature using the FE software ABAQUS/Standard.

2. Numerical model

2.1. Material modelling

Files must be in MS Word only and should be formatted for direct printing, using the CRC MS Word provided. Figures and tables should be embedded and not supplied separately. Concrete damage plasticity model (CDPM) available within ABAQUS/Standard was utilized in current model to simulate the performance and failure of the concrete material under ambient and elevated temperature. Further, the concrete crushing and concrete cracking are assumed as a basic failure criteria for concrete with compression and tension deterioration of material response being taken into consideration .Knowing that concrete was modelled as homogenous material. To simulate the plastic behaviour of concrete, the CDPM in

ABAQUS uses several parameters some of which are obtained from experimental tests. In the current model, the required plasticity parameters for the concrete materials are taken as assumed in ABAQUS and shown in **Table 1.**

Table 1 : Plasticity parameter used in current numerical model

Parameters	Assumed value	Parameters
Dilation angle Ψ	40	Dilation angle Ψ
Potential eccentricity ϵ	0.1	Potential eccentricity ϵ
fb0/fc0	1.16	fb0/fc0

The mathematical model of compressive stress-strain relationship of concrete that suggests by Eurocode 4 was adopted in current numerical model for ambient and elevated temperature. **Figures 2** shows graphical representations of the compressive behaviour of concrete at ambient and elevated temperatures according to Eurocode 4 [20]. To account for the reduction in the mechanical properties of concrete due to elevated temperature, compressive strength reduction factors obtained from the experimental tests conducted in current study was used as shown in Figure 2.

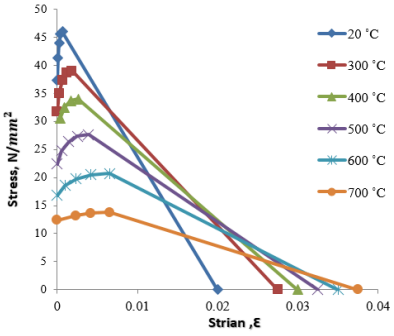

Figure 2: Stress - strain relationships of concrete at high temperature used in the numerical model of current study

For concrete under ambient and elevated temperature, tension stiffening was simulated in the numerical model through using fracture energy (Gf) (see **Figure 3**) .The value of Gf depending on the maximum aggregate size and the required concrete strength as presented in **Table 3.** Further, reduction factors of concrete tensile strengths results from the experimental tests was used in current model (see **Table 2**).

Table 2 : Results of tensile strength (ft) concrete cylinders under different elevated temperatures

Temp. ,˚C	$ft_{exp.}$, MPa	K_t Redaction factor
20˚C	2.4	/
300˚C	1.9	20%
400˚C	1.6	33.4%
500˚C	1.4	41%
600˚C	0.9	62.5%

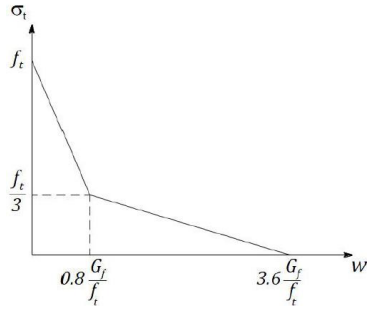

Figure 3: Bilinear softening tension of normal weight concrete used in current model (Hillerborg, 1985)

Table 3 : Values of Gf for different aggregate sizes and concrete strengths

$D_{max.,}$ mm	Gf (N/m)							
	C12	C20	C30	C40	C50	C60	C70	C80
8	40	50	65	70	85	95	105	115
16	50	60	75	90	105	115	125	135
32	60	80	95	115	130	145	160	175

The crack initiation and propagation of concrete crack at ambient and elevated temperature was simulate using the tension damage parameters (dt) which determined from equation 1 suggested by ABAQIUS (Hibbitt, 2008) as follows:

$$dt = 1 - \frac{\sigma t}{fctm} \quad (1)$$

On the other hand, the mathematical model of the stress-strain relationship of the reinforcing steel bars proposed by Eurocode 4 [20] was used in modelling the behaviour of the steel bars at ambient and elevated temperature. The modulus of elasticity and yielding stress of steel bars at ambient temperature were taken as 414 MPa and 2×10^5MPa respectively according to experimental tests. The reduction factors of reinforcing steel bars properties (yield strength, proportional limit and young modulus) at elevated temperature were taken from Eurocode 4 .

2.1 Material modeling of GFRP bars at ambient and elevated temperature

The mechanical properties of GFRP reinforcement bars provided by the manufactured company was used in the numerical model at ambient temperature. However, the reduction factors of the ultimate tensile strength and of elastic modulus of GFRP bars proposed by Saafi [1] was used in the numerical model to simulate the degradation of the mechanical characteristics of the GFRP bars at elevated temperature .Also ,the reduction factors of the specific heat ,density and thermal conductivity of GFRP bars proposed by Kodur et al. [3] was used in the numerical model as indicated in appendix A. Knowing that bar element was used to model the reinforcement with a 120 linear line element of type T3D2.

2.2 Geometrical modelling parameters

Three-dimensional eight-nodes solid with reduced integration hourglass control and reduced integration(C3D8R) available in ABAQUS/standard was used in current study to model the GFRP-RC beams, bearing plates as well as supporting plates during strucural analysis (see **Figure 4-a**). While, the eight-node solid linear with a temperature degree of freedom(DC3D8) was used in modeling the GFRP-RC beams, bearing plates and supporting plates in the heat transfer analysis. Furtheramore three-dimensional two nodes linear displacement truss element (T3D2) and a two nodes heat transfer link element (DC1D2) with a temperature degree of freedom were used in modeling of reinforcing GFRP and steel bars during structural and thermnal analyses respectively .Table 4 and Figure 4 show elements used in structural analysis and thermal analysis of current study.

Table 4: Element used in current numerical model

Structural analysis		Heat transfer analysis	
Part	**Type of element**	**Part**	**Type of element**
RC beams	C3D8R	RC beams	DC3D8
bearing plates, and supporting plates	C3D8R	bearing plates, and supporting plates	DC3D8
GFRP and Steel bars	T3D2	GFRP and Steel bars	DC1D2

a) C3D8R and DC3D8 elements **b) T3D2 and DC1D2 elements**

Figure 4 : Types of elements used in the current numerical model

2.3 Assembly of the numerical model

The assembly of all parts of GFRP-RC beams used by the present numerical model is shown in Figure 5. In order to preclude intensity of the stress at the supports and loading points, steel plates with dimensions of (150×80×10) mm and (150×100×10) mm (length ×width× depth) have been used as supporting and bearing plates respectively. To simulate the same boundary condition used in the experimental tests, displacement /rotation type of the boundary condition option available in ABAQUS was used. Further, the embedded region interaction option was used to simulate the interaction between reinforcement bars and concrete beams. Surface to surface tie interaction was used in simulating the relationship between GFRP-RC beams and bearing and supporting plates using the constraint option available in ABAQUS. **Figure 5** show the assembled parts of GFRP-RC beams.

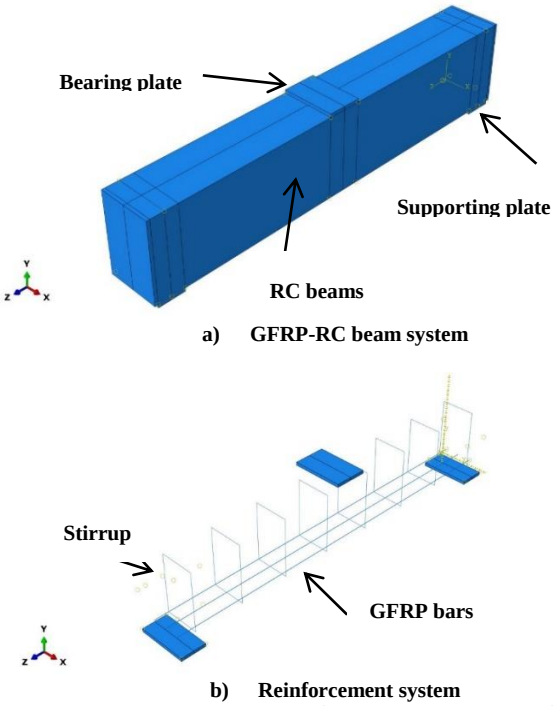

Figure 5: Schematic representation for the assembled parts of GFRP-RC beams

2.4 Analysis procedure

The sequential thermal-structural analysis procedure in ABAQUS/Standards was used in the current study to analyse the GFRP-RC beams exposed to elevated temperature followed by a static load. This analysis procedure includes two stages as follows:

2.4.1 Heat transfer analysis

In heat transfer analysis, the temperature was applied on a selected set of concrete external surface as a boundary condition in the heat transfer analysis step using the corresponding time –temperature history obtained from experimental tests (see **Figure 6**).The "Amplitude" option available in ABAQUS/standard was used to specify time–temperature histories from experimental tests.

2.4.2 Structural analysis

After completing the heat transfer analysis, structural analysis is initiated to obtain the structural performance of GFRP- RC beams after exposure to elevated temperature. A displacement controlled structural analysis was conducted by applying a lateral displacement as a boundary condition in the center of GFRP-RC beams using boundary condition option in ABAQUS

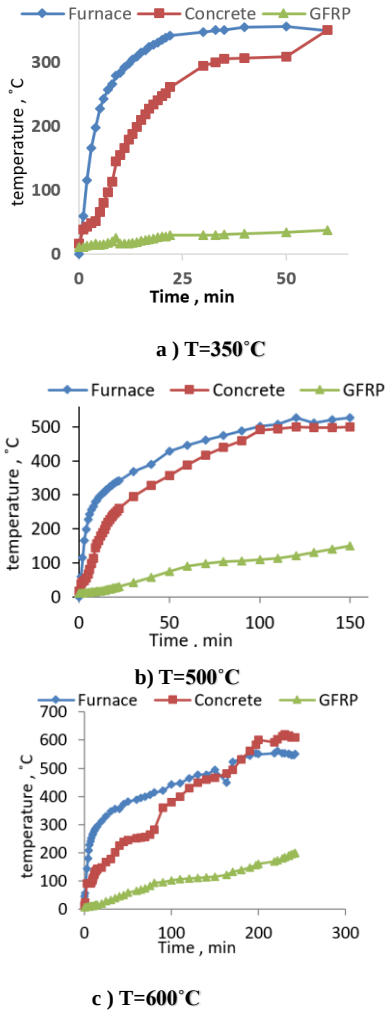

Figure 6: Time-temperature histories of experimental tested GFRP-RC beams under different temperatures

3. Validation of the numerical model

To ensure the reliability of the developed numerical model, experimental tests were carried out in this study on RC beams subjected to elevated temperature followed by concentrated static load at the beam's mid-span .The numerical simulation results obtained from the suggested model will be compared with the experimental tests results. The section below describes the experimental tests used in the validation of current numerical model.

3.1. Experimental test

Four GFRP-RC beams with cross-sectional dimensions of 250mm ×160 mm (width × height) and a total length of 1250 mm were designed according to ACI440.1R-15[12](see **figure 7**). All GFRP-RC beam specimens are made from normal weight concrete with an average compressive strength of 46 MPa .One beam specimens was tested at ambient temperature and the other three beams were firstly exposed to elevated temperatures of 350°C, 500°C and 600°C using electrical furnace then subjected to a monolithically increased load up to failure.

The internal dimensions of the furnace are 130×300×290 mm (length ×depth ×height) with maximum temperature of 900 °C was used to heat up the RC beam specimens .The average heating rate of the furnace is about 10°C /min and decrease gradually to the end of the heating process. An external thermocouple was attached to the specimens through a small hole in one long side of the furnace. Two thermocouples were used to measure and record the temperatures-time history at the concrete and at the GFRP bars. In addition, **Figure 8** show set up of electric furnace.

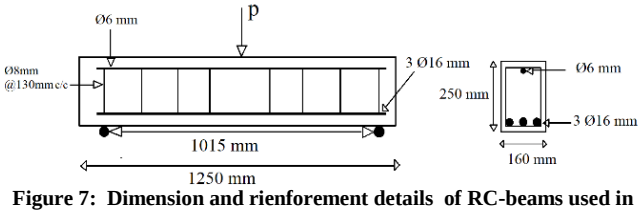

Figure 7: Dimension and rienforement details of RC-beams used in current study

(a)Electric furnace during thermal test (b) Thermally tested RC-beam

Figure 8 : Set up of the electric furnace

All GFRP-RC beams were tested using the universal testing machine obtained at the structural laboratory of College of Engineering/ The University of Al-Qadisiyah. Deflection at mid span corresponding to each load increment during the structural tests was monitored and recorded using a linear variable displacement transducer (LVDT) with a maximum capacity of 50 mm.

3.2. Validation of the numerical model against thermal tests

The results obtained from heat transfer analysis were presented in terms of temperature - time- histories at the surface of main reinforcement GFRP bars and compared with temperature - time- histories of corresponding experimental thermal tests as shown in **Figure 9** .The comparisons show reasonable agreement between the numerical simulation results and the experimental tests results especially at maximum temperature transferred from concrete to the GFRP bars. This agreement indicates the accuracy of the suggested model in capturing the temperature distribution inside the concrete cross-section. In addition, Figure 9 clearly shows that as the distance from concrete surface increased the corresponding temperature is considerably decreases.

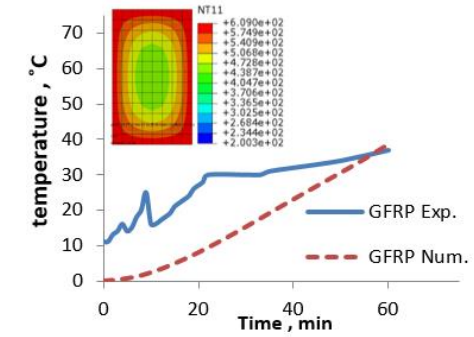

a) **Under 350 ºC**

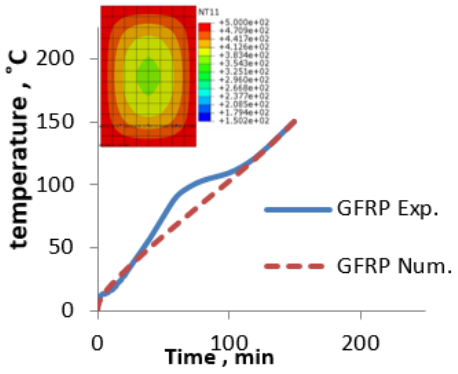

b) Under 500 ºC

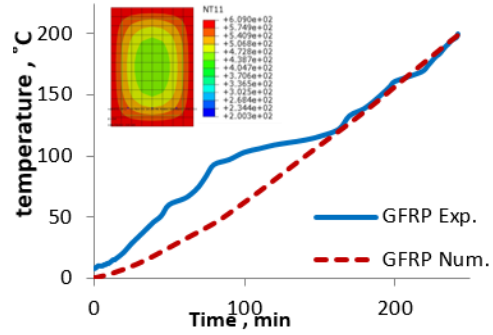

c) Under 600 ºC

Figure 9 : Temperature- time histories at the surface GFRP bars of the tested beam

3.3. Validation the numerical model against the structural tests

The results of numerical model in terms of ultimate load-lateral displacement relationships of GFRP-RC beams were compared with the corresponding experimental load-displacement relationships .**Figures (10-a-d)** illustrate the comparison for GFRP RC beams. Good agreement can be seen between the two sets of results. This agreement confirms that the proposed numerical model have the ability to estimate and predict the response and maximum load of GFRP- RC beam under different elevated temperatures up to failure. Numerical simulation results reveal that the maximum load of GFRP-RC beams was found to be decreased by 1%, 8%, and 9% compared to the maximum load of control beam under exposure to a temperature of 350, 500, and 600 ºC respectively (see Figure 10 and Table 5).Furthermore, Table 5 shows comparison of failure load between numerical model and experimental tests Comparison indicated very reasonable agreement can be seen between the two results.

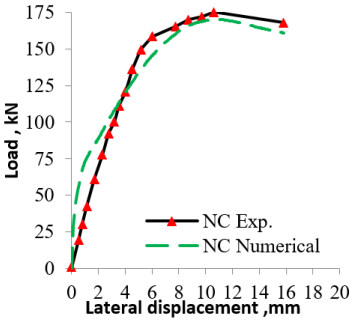

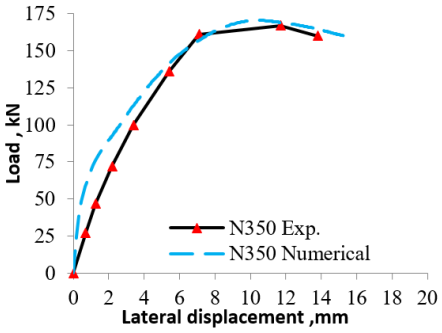

a) **NC**

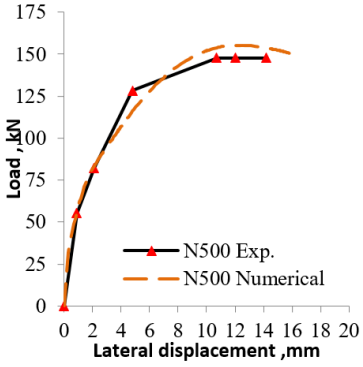

b) N350

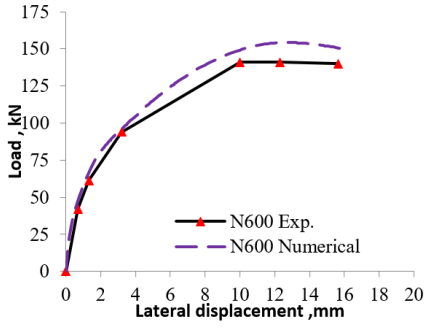

c) **N500**

d) N600

Figure 10 : Numerical versus experimental load-displacement relationship of GFRP-RC beams exposed to different elevated temperatures.

Table 5 : Comparison of failure load between numerical model (Abaqus) results and conducted experimental results of GFRP-RC beams under exposure to high temperature.

Beam designation	Ultimate load(kN)-Experimental	Ultimate load(kN) Abaqus	% Difference between exp. and num. results
NC	174	170	2%
N350	167	170	1.7%
N500	147	155	5%
N600	141	154	8.4

4. Parametric study

The validated numerical model was utilized to carry out a parametric investigation to demonstrate the effect of two important parameters on the performance GFRP reinforced concrete beams exposed to an elevated temperature which have not addressed in the current experimental study these parameters as follows:

(a) Effect of temperature - time history.
(b) Effect of temperature distribution around the cross-section of the GFRP-RC beams.

4.1. Effect of temperature distribution around GFRP-RC beams

A temperature value of 600 ºC was considered in the current parametric study with three cases of temperature distribution: one side temperature exposure at the top layer of the section, one side temperature exposure at the bottom layer of the section and three sides temperature exposure in addition to the four sides exposure which is previously analyzed as shown in **Figure 11**. Load -displacement relationships of the beam N600 under above selected cases of thermal exposure were shown in **Figure 12**. Top section, bottom section and three sides' temperature exposure results revealed increasing in maximum load by 11.5%, 13% and 13% respectively compared to maximum load of the beam N600 obtained from experimental test. The reason for this increase may be attributed to the resistance of unheated and undamaged layer of beam. The un-heated and un-damaged layer of the beam can resist more loading capacity than all heated beam layers due to un-deterioration of mechanical characteristic of unheated concrete and reinforcement bars.

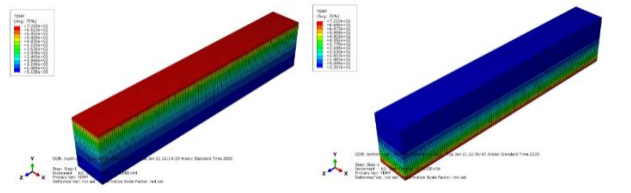

a) Top layer exposure **b) Bottom layer exposure**

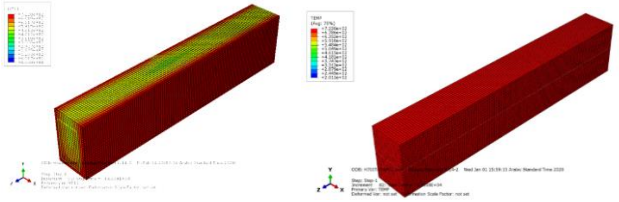

c) Three side exposure **d) all side exposure**

Figure 11 : Temperature distribution around GFRP-RC beam

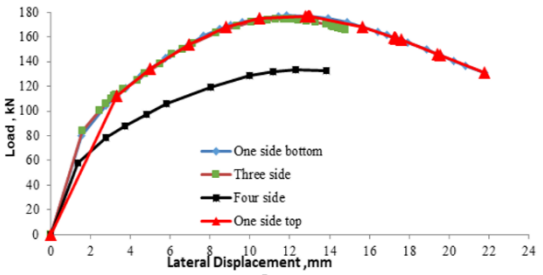

Figure 12 : Load -displacement relationships of N600 beam under different temperature distribution around beams

4.2. Effect of temperature distribution along the GFRP-RC beams

The investigated beam length was as follows: half-length exposed and three-quarter length exposed in addition to the full length exposure which is previously analysed of N600 beam as shown in **Figure 13**.The load-displacement curves are shown in **Figure 14**. The results of half exposed length shows increasing in ultimate load capacity by 7% compared to ultimate load capacity of full length exposure While, the results of three-quarter length exposed shows very little decreased in ultimate load capacity by about 1% compared to ultimate load capacity of full length exposure case of N600 beam obtained in experimental study (see **Figure 14**). This difference in the ultimate load capacity is due to the influence of high-temperature exposure on the mechanical characteristic of the exposed length of GFRP-RC beam.

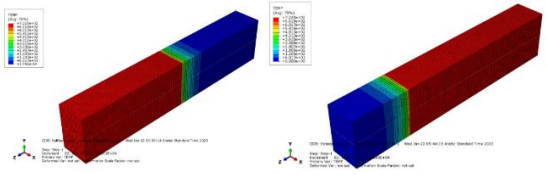

a) **Half-length exposure** **b) Three-quarter length exposure**

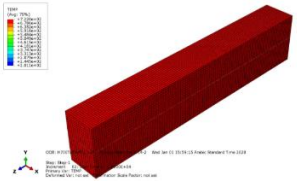

c) Total length exposure

Figure 13 : Temperature distribution along GFRP-RC beam

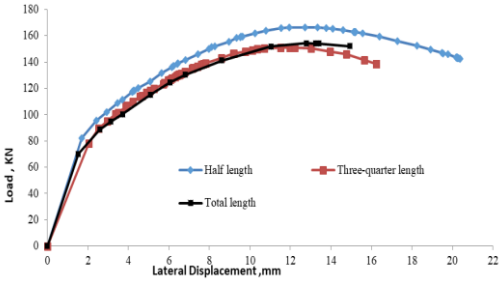

Figure 14 : Load -displacement relationships of N600 beam under different temperature distribution along the beams.

5. Conclusions

The main conclusions and findings extracted from the numerical simulations carried out in this study were summarized as follows:

1. The finite element software ABAQUS/Standard can reasonably predict the performance and ultimate load of GFRP-RC beams under different elevated temperatures if suitable geometrical, thermal dependent material and mechanical properties are selected and implemented correctly.
2. The distribution of the temperature around the GFRP-RC beam has a considerable effect on ultimate load of GFRP-RC beam. At the temperature of 600°C, when the temperature is distributed above one side (top section) , one side (bottom section) and three sides ,ultimate load capacity increased by 11.5%, 13% and 13% respectively
3. The distribution of the temperature over the length of GFRP reinforced concrete beam has reflected a slight effect on the maximum capacity of GFRP-RC beams. At temperature value of 600°C, the numerical results of the half temperature exposed length shows increasing in ultimate load by 7% compare with maximum load of full-length temperature exposure. While, the results of three-quarter length exposed shows very little decreased in ultimate load capacity by 1 %.

REFERENCES

[1] M. Saafi, Effect of fire on FRP reinforced concrete members, Compos. Struct. vol. 58, no. 1, pp. 11–20, 2002.

[2] M.Rafi, A. Nadjai, Finite element modeling of carbon fiber-reinforced polymer reinforced concrete beams under elevated temperatures, ACI Struct. J., vol. 105, no. 6, pp. 701–710, 2008.

[3] B.Yu , V.K.R. Kodur, Factors governing the fire response of concrete beams reinforced with FRP rebars, Compos. Struct. vol. 100, pp. 257–269, 2013, doi: 10.1016/j.compstruct.2012.12.028.

[4] A. Abbasi, PJ. Hogg, A model for predicting the properties of the constituents of a glass fibre rebar reinforced concrete beam at elevated temperatures simulating a fire test, Compos. Part B Eng., vol. 36, no. 5, pp. 384–393, 2005.

[5] M. Sakashita , Y. Masuda, K. Nakamura , H. Tanano , Deflection of continuous fiber reinforced concrete beams subject to loaded heating in non-metallic (FRP) reinforcement for concrete structures, proceedings of 3th international symposium, Japan Concrete Institu, 1997.

[6] T.D. Lin, B. Ellingwood and O. Piet, Flexural and shear behaviour of reinforced concrete beams during fire tests, U.S. Department of Commerce National Bureau of Standards Centre of Fire Research Gaithersburg, MD 20899; November , 1988.

[7] M. Al-Baghdadi, Effect of High Temperature on Some Properites of Light Weight Concrete, MATEC Web Conf., vol. 138, no. 2, p. 01007, 2014.

[8] ISO 834. Fire resistance tests elements of building construction. International Organization for Standardization; 1975. 1999.

[9] A. Abbasi , Behaviour of GFRP-RC elements under fire condition, PhD thesis, Queen Mary, University of London; June 2003, 2003.

[10] M. Rafi, A. Nadjai and F. Ali, Finite element modelling of carbon fiber-reinforced polymer reinforced concrete beams under elevated temperatures, ACI Struct. J., vol. 105, no. 6, pp. 701–710, 2008.

[11] Eurocode 2.Design of concrete structures"Part 1-2: General rules Structural fire design Euro code SS-EN-1992-1-2:2008, 3(July)., Eurocode 2, vol. 2, 2004.

[12] A. Nanni, Guide for the design and construction of concrete reinforced with FRP bars (ACI 440.1R-03). 2005.

[13] T.T. Lie. , Structural Fire Protection. American Society of Civil Engineers Manuals and Reports on Engineering Practice No. 78. ASCE, New York, NY. 1992.

[14] L. A. Bisby, Fire behaviour of fiber-reinforced polymer (FRP) reinforced or confined concrete by in conformity with the requirements for the degree of Doctor of Philosophy, no. August, p. Fire behaviour of fiber-reinforced polymer (FRP) r, 2003.

[15] T.T. Lie, RJ. Irwin, Method to calculate the fire resistance of reinforced concrete columns with rectangular cross section. ACI Struct J 1993; 90(1):52–60., 1993.

[16] Y.C. Wang, V.K.R. Kodur, Variation of strength and stiffness of fibre reinforced polymer reinforcing bars with temperature, Cem. Concr. Compos. vol. 27, no. 9–10, pp. 864–874, 2005.

[17] F. Bulletin. FRP reinforcement in RC structures.Fédération Internationale du Béton, Lausanne, Switzerland; 2007.

[18] M. Rafi, A. Nadjai and F. Ali, Fire resistance of carbon FRP reinforced concrete beams. J.ournal of Advanced Concrete Technology Vol. 6, No. 3, 431-441, 2008.

[19] A. Abbasi, PJ.Hogg, Fire testing of concrete beams with fiber reinforced plastic rebar. Composites: Part A 37 (2006) 1142–1150, Compos. Part A :Appl. Sci. Manuf., vol. 37, no. 8, pp. 1142–1150, 2006, doi: 10.1016/j.compositesa.2005.05.029.

[20] Eurocode 4. Design of composite steel and concrete structures–„EN 1994.Part 1-2: General rules - Structural fire design, (August), pp. 1-109, Des. Compos. Steel Concr. Struct. – Part 1-2 Gen. Rules - Struct. Fire Des. no. August, 2005.

[21] R. Hawileh, A. Naser, Thermal-stress analysis of RC beams reinforced with GFRP bars, Compos. Part B Eng., vol. 43, no. 5, pp. 2135–2142, 2012, doi: 10.1016/j.compositesb.2012.03.004.

[22] I. Hibbitt, Karlsson and Sorensen, ABAQUS. ABAQUS standard user's manual. Vol. I-III, Version 6.8. Pawtucket, 2008.

Appendix A

Table A.1: Reduction factor of mechanical properties of GFRP bars

Tensile Strength[1]	$k_f=\frac{f_{fu,T}}{f_{fu,20°C}}$, (T in °C) k_f=1-0.0025 T for $0\leq T\leq 400$ k_f=0 T for $400\leq T$
Modulus of Elasticity [1]	$k_E=\frac{E_T}{E_{20°C}}$, (T in °C) k_{fE}=1 for $0\leq T\leq 100$ k_{fE}=1.175-0.00175 T for $110\leq T\leq 300$ k_{fE}= 1.625-0.00325 T for $300\leq T\leq 500$ k_E=0 for $500\leq T$
Specific Heat [3]	C=$(1.25+\frac{0.95}{325}T)\times 10^3$ For 20℃ ≤ T ≥ 325℃
Thermal Conductivity[3]	$K_{f,T}=1.4+\frac{-1.1}{500}$ T For 20℃ ≤ T ≥ 500℃
Density [3]	ρ= ρ(20℃)= $Reference\ density$ For 20℃ ≤ T ≥ 510℃